International Journal of Adhesion & Adhesives 117 (2022) 103168

Contents lists available at ScienceDirect

International Journal of Adhesion and Adhesives

journal homepage: www.elsevier.com/locate/ijadhadh

High clarity polyurethane laminating adhesives based on poly (propylene glycol). Effect of hard segment on microphase morphology, haze and adhesion

S. McCreath [a], P. Boinard [b], E. Boinard [b], P. Gritter [b], J.J. Liggat [a,*]

[a] WestCHEM, Department of Pure and Applied Chemistry, University of Strathclyde, Glasgow, Scotland, UK
[b] Block 7, Vale of Leven Industrial Estate, Dumbarton, Dunbartonshire, Scotland, UK

ABSTRACT

Within this publication, the performance of high clarity polyurethane adhesives based on a poly(propylene glycol) soft-phase within a polycarbonate or ethanolamine surface-treated polycarbonate laminate, is described. A series of polyurethanes were prepared, with poly(propylene glycol) used as soft-phase due to the high clarity of this polyol and absence of carbonyl functionality, which allows for hard-phase architecture to be resolved with greater resolution. In total, eight adhesives were synthesised, each contained a different chain-extender formulation to gauge what influence hard-phase architecture had on laminate haze and peel strength. This was investigated using either 4,4-methylene diphenyl diisocyanate or isophorone diisocyanate as hard-phase with trimethylolpropane as the only chain-extender or by including one of the following sterically hindered diols: 2,2-diethyl-1,3-propane diol, 1,3-butane diol or 1,2-proane diol. DSC analysis showed that microphase morphology was strongly influenced by the diisocyanate present, as shown by the degree of phase mixing being greater in methylene diphenyl diisocyanate based formulations when compared with isophorone diisocyanate based. ATR complements this observed difference in microphase morphology, with isophorone diisocyanate based formulations having a greater composition of hydrogen-bonded urethane and urea functionality present within the hard-phase which displays a more phase separated composition. Interestingly, differences in microphase mixing did not have a consistent influence on the peel strength obtained, with only 31% of laminate combinations tested recording a peel strength of <3 N mm^{-1} after 18 months. Diol chain-extended formulations based on methylene diphenyl diisocyanate accounted for 25% of these lower values and was a consequence of their poorer process-ability during lamination. This resulted in higher haze values being encountered for both polycarbonate and ethanolamine surface-treated polycarbonate laminates which contained methylene diphenyl diisocyanate based formulations when compared to isophorone diisocyanate based formulations, where all values were $<1.5\%$.

1. Introduction

Polyurethane adhesives are a diverse class of polymer which are fundamentally based around the formation of urethanes linkages, however, it is possible to incorporate many different types of chemical functionalities into these materials. Consequently, polyurethane adhesives are found in a variety of different industries which include (but not limited to) construction, medical, automotive and aerospace [1,2]. A distinguishing quality of polyurethanes which facilitates their appearance in many industries is the ability to obtain custom-made properties to suit almost any application. This makes it possible to formulate an adhesive which possess the necessary mechanics required of a tough structural adhesive for construction or conversely the soft elastomeric properties required for lamination [3,4].

Currently, great efforts are being made to move towards water-based or solvent-free formulations as regulatory pressure is pushing for solvent-based formulations of reduced volatile organic content, however, this transition is not without its issues [5]. A common issue that is limiting the implementation of water-based adhesives is the extended drying time required when compared to solvent-based adhesives [6]. Solvent-free adhesives are not without their problems either, as their inherent high viscosity can often affect surface wetting and final adhesion [7]. This can be overcome by applying the adhesive at elevated temperature, however, this has additional safety concerns associated with handling high temperature molten material.

In a previous publication, solvent-free, moisture-cured polyurethane adhesives were developed for lamination of polycarbonate and ethanolamine treated polycarbonate laminates [8]. A solvent-free approach was selected over water-based to reduce the time required between application and lamination. It was shown that hard-phase to soft-phase miscibility had an impact on the observed final microphase morphology, adhesion and optical clarity of the adhesive. It was demonstrated that using an aromatic isocyanate based hard-phase with sterically hindered chain-extenders increased microphase mixing which subsequently

* Corresponding author.
E-mail address: j.j.liggat@strath.ac.uk (J.J. Liggat).

https://doi.org/10.1016/j.ijadhadh.2022.103168
Received 20 January 2022; Accepted 14 April 2022
Available online 20 April 2022

retarded crystallisation of the polyester soft-phase. When an aliphatic based hard-phase was used, the microphase morphology displayed greater degrees of phase separation and this allowed for crystallisation of the soft-phase to occur.

To develop on these findings, the current publication will focus on using a fully amorphous soft-phase. Poly(propylene glycol) (PPG) was selected due to its amorphous nature and the absence of any carbonyl functionality, which aids the interpretation of final hard-phase architecture. Two hard-phase diisocyanates were selected for evaluation, namely methylene diphenyl diisocyanate (MDI) and isophorone diisocyanate (IPDI). Using these materials, eight polyurethane (PU) prepolymer adhesives were prepared and studied. Each diisocyanate set contained a base formulation containing triol chain-extender trimethylol propane (TMP) only. To investigate chain-extender effects on morphology, three additional formulations containing a combination of TMP with either 2,2-diethyl-1,3-propane diol (DEPD), 1,3-butane diol (BD) or 1,2-propane diol (PD) (chain-extender structures shown in Fig. 1) were synthesised.

All adhesives were laminated at a thickness of 50 μm between two plies of 175 μm polycarbonate and allowed to moisture cure at ambient temperature. Characterisation of each moisture cured polyurethane-urea (MCPU-U) was performed by attenuated total reflectance Fourier transform infrared spectroscopy, differential scanning calorimetry and thermal gravimetric analysis. Peel strength measurements of untreated and ethanolamine surface treated polycarbonate for each adhesive was tested by the 180° T-peel method. Haze measurements of each adhesive within the polycarbonate laminates were investigated using a light diffusion technique.

2. Experimental

2.1. Materials

The following materials were purchased from Sigma-Aldrich® and used as received: 4,4-MDI, IPDI, dibutyltin dilaurate (DBTDL), triethylamine (TEA), isopropyl alcohol (IPA) and ethanolamine (EA). TMP, DEPD, BD, PD and 1000 molecular weight PPG were all from Sigma-Aldrich®, and were dried at 80 °C under vacuum prior to use. 175 μm thick bisphenol-A polycarbonate (PC) film was supplied by Sabic.

2.2. Prepolymer synthesis

Prepolymer synthesis was performed within a reaction kettle equipped with a nitrogen inlet, nitrogen outlet, over-head mechanical stirrer, k-type thermocouple and reactant addition inlet. The polyurethane (PU) prepolymer synthesis was carried out in either one or two synthetic steps as shown in Scheme 1 for MDI and Scheme 2 for IPDI.

In step-one, a mixture of PPG with 10 mol% of triol chain-extender TMP was added to the reaction kettle (calculated from moles of OH in PPG) and allowed to equilibrate at 90 °C ± 5 °C for 30 min with constant stirring. Next MDI or IPDI was added at a 2.2:1.0 stoichiometric ratio (NCO:OH). To control the reaction exotherm and ensure that the temperature did not exceed 95 °C, diisocyanates were added in 1 ml portions. Note that MDI is a solid and had to be melted in a separate vessel at 50 °C under an atmosphere of nitrogen prior to being added to the main reaction kettle. Once all the diisocyanate had been added, the reaction was left to stir for 3 h for MDI-based adhesives and 5 h for IPDI-based adhesives. The TMP-only formulation was complete at this stage and and after the addition of curing catalysts at 0.1 wt% of the total batch weight (0.05 wt% TEA, 0.05 wt% DBTDL) and degassing under vacuum at 50 °C, the sample was transferred to an aluminium cartridge that was stored at 5 °C under vacuum until application.

In synthetic step two, the prepolymer was chain-extended with one of the low-molecular weight diols. The NCO:OH addition ratio for chain-extender was 2.2:1.0 and was based on the calculated free isocyanate content remaining after step one. Following addition of chain-extender, the reaction was held at 90 °C ± 5 °C with constant stirring for 5 h when MDI-based or 19 h when IPDI-based. Next, the curing catalysts (0.05 wt % TEA, 0.05 wt% DBTDL) were added and the sample degassed as above. The PU prepolymer was then transferred to an aluminium cartridge and stored under vacuum at 5 °C until application. Formulations were used within one month of synthesis.

2.3. PC surface treatment

Each PC film was surface treated using a 70:30 treatment solution consisting of IPA:EA and was based on a study by Wilkes et al. [9]. The treatment solution was applied by wiping over the films surface for 2 min, followed by a 1 min rest period to allow solvent evaporation and then placed within a 120 °C oven for 2 min. Once removed from the oven, surface treatment was complete and films were ready for adhesive application.

2.4. Adhesive application

Adhesive application was carried out using a heat gun applicator into which the aluminium cartridge containing the formulation was inserted. Application temperatures were formulation dependent and ranged between 95 °C–150 °C in MDI-based or 95 °C–105 °C in IPDI-based adhesives. Two different laminate combinations were prepared consisting of PC to PC and PC(t) to PC(t) ((t) denotes surface treated). The adhesive was applied to the bottom substrate prior to both plies passing through a set of steel nip rollers with a fixed gap to leave a 50 μm adhesive thickness. Lamination was driven by a second set of rubber rollers from a ChemInstruments laboratory LL-100 laminator which was set to 1 m min^{-1} with a clamping pressure of 20 psi. Following lamination each sample was cured flat at ambient temperature.

2.5. Attenuated total reflectance Fourier transform infrared spectroscopy (ATR)

Analysis was carried out on an Agilent Technologies 4500 Series Portable FTIR Spherical Diamond ATR. Each spectrum consisted of 128 scans at a resolution of 8 cm^{-1} with the sampling depth around 2 μm at 1000 cm^{-1}. Characterisation of each adhesive using ATR was obtained on 30-day-old 180° T-peel samples. Analysis of each laminate was carried out at nine random positions along the sample length. These nine spectra were then averaged to determine the variation within the

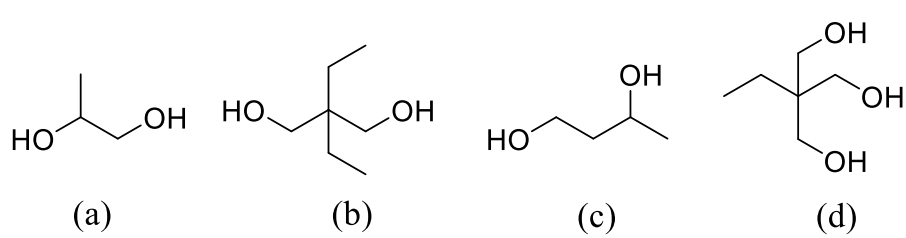

Fig. 1. Structure of chain-extender used during synthesis. (a) 1,2-propane diol, (b) 2,2-diethyl-1,3-propane diol, 1,3-butane diol and trimethylol propane.

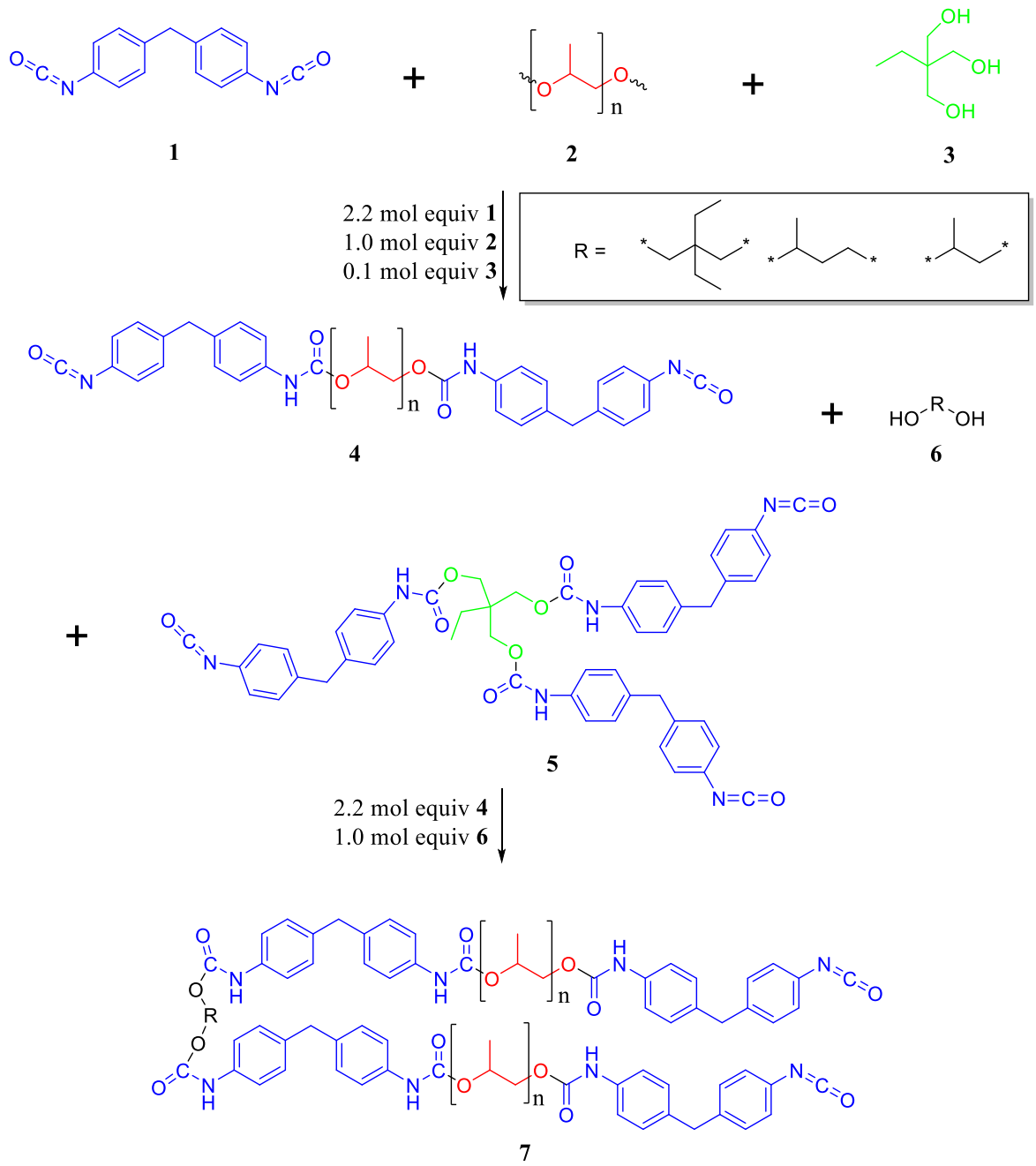

Scheme 1. General reaction scheme for the synthesis MDI and PPG based chain-extended polyurethanes adhesives. 1 = MDI, 2 = PPG, 3 = TMP, 4 = MDI-PPG prepolymer, 5 = end capped MDI-TMP, 6 = chain-extender and 7 = chain-extended prepolymer.

adhesive layer. ATR spectral averaging was carried out using LabCognition® Panorama and spectra plotted using Originlab OriginPro® 9.0. Deconvolution of the N–H and C=O regions was performed using OriginPro® 9.0 software using the Gaussian fitting function tool.

2.6. Differential scanning calorimetry (DSC)

DSC experiments were carried out using a TA Q1000 differential scanning calorimeter. Analysis of MCPU-Us typically involved 5–10 mg of sample within a hermetically sealed aluminium pan. Samples were analysed following 1 month of ambient temperature cure. Experiments were performed under a nitrogen gas flow of 40 ml min^{-1}, a heating rate of 10 °C min^{-1} and a cool-heat-cool-reheat procedure. Samples were initially cooled to −90 °C and heated to 150 °C in order to remove any thermal history from the sample. Samples were next re-cooled to −90 °C and then heated to 300 °C. To allow sample exposure to the purge gas, the lid of the aluminium pan was pierced prior to the experiment being carried out. All experimental data were analysed with TA's thermal analysis software and plotted using OriginPro® 9.0.

Nominal hard-phase contents (wt%hp) for each formulation were calculated using equation (1):

$$wt\%hp = \frac{((R)(M_{hp}) + (R-1)(M_{ce})}{(M_{sp} + R(M_{hp}) + (R-1)(M_{ce})} \quad (1)$$

R = stoichiometry of diisocyanate to polyol, M_{hp} = mass of diisocyanate used in hard-phase, M_{ce} = mass of chain-extender(s) used in hard-phase and M_{sp} = number average molecular weight of PPG [10].

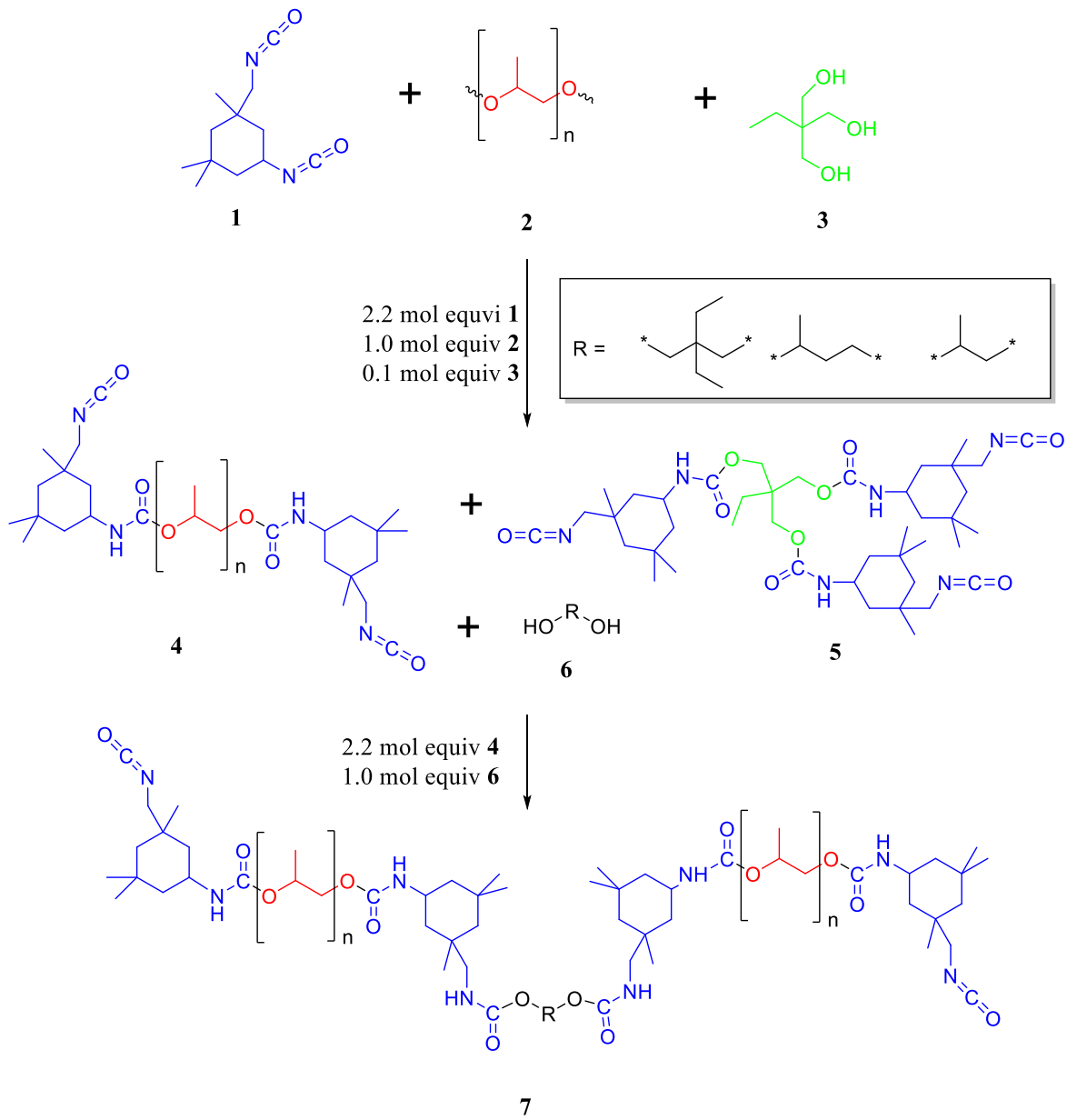

Scheme 2. General reaction scheme for the synthesis of IPDI and PPG based prepolymer adhesives. 1 = IPDI, 2 = PCD, 3 = TMP, 4 = isocyanate end capped prepolymer of PPG, 5 = isocyanate end capped prepolymer of TMP, 6 = diol chain-extender and 7 = diol chain-extended prepolymer.

2.7. 180° T-peel testing

180° T-peel testing was carried out using an Instron 4301 equipped with a 1 kN load cell. Experimental parameters were fixed at 25 mm sample width, 150 mm extension length and 100 mm min^{-1} extension rate. Samples were tested at three intervals following lamination, namely 1 week, 1 month and 18 months. Following 1 month of cure, the target peel strength was 3 N mm^{-1} and this value was to be maintained following 18 months. Peel strength was calculated from the data between 50 mm and 150 mm. Data from the first 50 mm was not included in the calculation as peel stability was being established within this region. Peel strength values were then calculated using equation (2).

$$P = \frac{L}{w}(1 - \cos\theta) \tag{2}$$

P = peel strength in N mm^{-1},
L = load in N,
w = sample width in mm,
θ = peel angle in degrees.

As the peel angle used within this study was 180°, equation (2) reduces to:

$$P = \frac{2L}{w} \tag{3}$$

The values obtained are the average of three sample replicates.

2.8. Haze determination

The haze of each MCPU-U was tested using a BYK Gardner® Hazegard Dual light diffusion technique. The value quoted for each adhesive is an average obtained from five haze test replicates. The test employed measures transmittance and deviation angle of the incident

beam by the laminated material. Haze data was analysed in accordance with ASTM D1003.

Testing was performed by placing each laminate sample in the path of a narrow beam of incident light. As this incident beam passes through the material it will either pass through unimpeded or be diffusely scattered. Both these parts of the beam then enter an integration sphere equipped with a photodetector. From this collected light, two quantities can be determined: the total strength of the light beam and the portion of the original beam that has been deviated by an angle of >2.5°. Obtaining these two quantities allows for calculation of both haze which is calculated from the wide-angle diffuse component and luminous transmittance which is the percentage of the incident beam that has been transmitted through the sample unimpeded. The target haze value for each laminate is <1.5% to ensure high clarity is obtained.

3. Results and discussion

3.1. DSC analysis

3.1.1. DSC of MDI adhesives

Discussion of the thermal behaviour for adhesive formulations based on MDI and PPG as evaluated by DSC will be discussed first. Within Table 1, thermal data collected for all four formulations is presented. We restrict our interpretation to the region below 175°C as TGA data (see SI) indicates that mass-loss, indicative perhaps of degradation, occurs for some formulations above this temperature. Beginning with $T_g$sp (soft-phase glass transition temperature) of PPG, the observed position for this transition was −70 °C and spanned a narrow range of 2 °C (data not shown). Having such a sharp glass transition which occupies a narrow range is typical of low molecular weight polymers of low polydispersity that contains a sterically hindered backbone structure [11].

Fig. 2 displays the DSC curves of each cured adhesive obtained on the second heating cycle. For MDI-TMP-PPG, the glass transition has shifted by +62 °C compared to PPG and occurs at −8 °C. This shift is coupled with visible broadening and the occupied range now covers 14 °C from −18 °C to −4 °C. A shift to higher temperature in $T_g$sp can be observed for each diol chain-extended adhesive, with 7 °C reached for DEPD, 1 °C reached for BD and 1 °C reached for PD when compared to the TMP only chain-extended formulation. Again, accompanying each elevated $T_g$sp was an increased transition width.

Elevation of $T_g$sp following the introduction of each sterically hindered diol displays that chain-extension further facilitates mixing of the hard and soft-phases. This indicates that diol chain-extenders of this type, improve the miscibility of soft and hard-phases. These observations complement what has been suggested within the literature, it is indeed a combination of chemical compatibility, hard-phase block length and disorder introduced by sterically encumbered chain-extenders that can shift microphase morphology towards phase-mixing over self-aggregation [4].

Observed shifts and broadening of the glass transition due to phase-mixing complements what has been observed elsewhere within the literature for MCPU-Us containing a polyether soft-phase [12,13]. As the hard-phase becomes dissolved within the soft-phase, the mobility of polymer chains is reduced due to newly introduced conformational constraints in the form of physical cross-links. These physical cross-links occur due to hydrogen-bond formation between the hard and soft-phases of the material [12]. The introduction of this additional structure effectively increases polymer molecular weight during cure and contributes towards the elevation and broadening of the $T_g$sp [11].

Table 1
DSC data obtained during second heating scan of each MCPU-U containing MDI and PPG.

Formulation	HS wt%	$T_g$sp/°C
PPG	–	−70
MDI-TMP-PPG	36.4	−8
MDI-TMP-PPG-DEPD	41.5	7
MDI-TMP-PPG-BD	40.0	1
MDI-TMP-PPG-PD	39.5	1

HS = nominal hard-phase content, $T_g$sp = soft-phase glass transition temperature second heating scan.

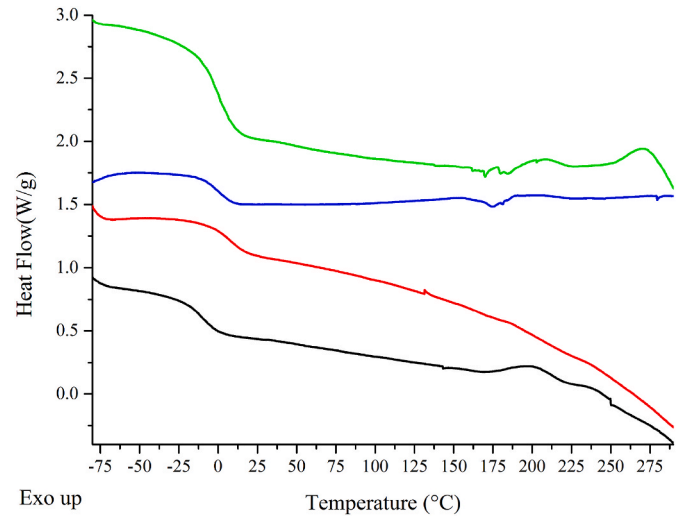

Fig. 2. Stacked DSC curves from the second heating cycle for MCPU-U adhesives based on MDI and PPG. [MDI-TMP-PPG in black, MDI-TMP-PPG-DEPD in red, MDI-TMP-PPG-BD in blue and MDI-TMP-PPG-PD in green].

In a paper by Ryan et al., it was discussed how precipitation of chain-extenders within the hard-phase can affect the packing arrangement and overall segmented structure [14]. Precipitation in this sense is defined as "upon matrix solidification chain-extender molecules will be segregated or phase separated within the hard-segment only, directly affecting this segment's crystalline structure" [14]. Therefore, chain-extender precipitation will have an influence not only on the packing of the hard-phase but also on the miscibility of the hard-phase and soft-phase.

This interpretation of chain-extender precipitation within the hard-phase of the network was used during the design of current formulations. Therefore, the actual hard-phase content will be dependent on the post-polymerisation morphology. For the current formulations, it was anticipated that this will be disrupted due to the structures of the chain-extenders, which will influence the morphology post moisture cure. The success of this strategy will be discussed during the haze interpretation of these formulations when part of laminated structures.

Sànchez-Adsuar et al. and Gisselfält et al. reported that chain-extender length and structure has an impact on the microphase morphology, with short chain-extenders promoting ordered hard-phase packing along with phase separation [15,16]. Within that study ethylene glycol, 1,4-butane diol and 1,6-heaxane diol were used during synthesis. It was shown through monitoring the position of the $T_g$sp by DSC, that 1,6-hexane diol displayed the greatest shift due to microphase mixing. As the diol chain-extenders used within this study contain side groups (ethyl in DEPD and methyl for BD and PD), it is anticipated that these will interfere with the intimate packing of the hard-phase, which is consistent with observations of Gisselfält et al. [16].

Based on the literature for segmented block copolymers it would be expected to observe a glass transition of the hard-phase [12,17,18]. For formulation MDI-TMP-PPG, two small higher temperature thermal transitions were observed. The first transition occurs at 32 °C and is associated with dissociation or relaxation of hard-phase blocks that are highly disordered. This transition may correspond to hard-phase domains that contain TMP, as this chain-extender has a known disruptive effect [19]. Observation of these weak transitions is difficult but becomes clearer when the first derivative of heat flow is plotted for the second heating cycle (see supplementary information).

Further identified following first derivative treatment of the heat flow was the $T_g$hp for more ordered domains at 81 °C. This value is consistent with the literature for formulations of similar hard-phase content and short hard-phase block length [20]. Of the diol chain-extended formulations, only MDI-TMP-PPG-DEPD displays a $T_g$hp at 96 °C [12]. As the glass transition has shifted to a higher temperature, it suggests that the greater hard-phase block length introduced by diol chain-extenders promotes hard-phase aggregation over that of the triol chain-extender only, however, it is noted that these transitions are very small.

Returning to the statement made by Ryan et al., namely that precipitation of the chain-extender within the hard-phase directly affects the packing arrangement and the ability to crystallise, this is consistent with the current data set [14]. Further contributing towards this hard-phase disruption is the triol chain-extender TMP that was kept constant at 15 mol% of the total chain-extender content. Work by Petrović et al. reported that incorporation of TMP into the hard-phase serves to reduces crystallinity as inhomogeneity is introduced into the packing arrangement [13]. It was reported that when TMP of 15 mol% or greater is used, the hard-phase crystallinity was compromised. From DSC data collected on the current adhesive set, it is clear that TMP has influenced hard-phase packing. Evidence of MDI end-capped prepolymers of TMP were identified by MALDI-ToF-MS (matrix assisted laser desorption ionisation time of flight mass spectrometry) and as a result these moieties will be present within both urethane/urea hard-phases (mass spectra shown in supplementary data).

3.1.2. DSC of IPDI adhesives

Fig. 3 displays the curves collected during the second heating cycle for formulations based on IPDI and PPG, with data within Table 2. Visible from inspection of Fig. 3 is that all four materials only display a single glass transition. This glass transition is of the soft-phase PPG and has been elevated in temperature by around 40 °C which displays that phase-mixing has occurred. It is noted that the value of each $T_g$sp is similar, indicating that the influence of the chain-extender on the miscibility of IPDI and PPG is small. Therefore, it would be expected that any changes to the hard-phase architecture will have minimal effect on the final morphology. This is consistent with observations made in previous work on IPDI-based adhesive systems [8].

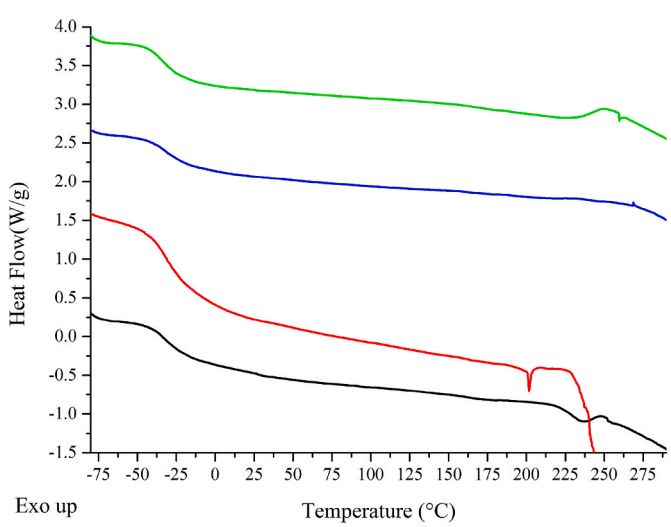

Fig. 3. Stacked DSC curves from the second heating cycle for each MCPU-U. [IPDI-TMP-PPG in black, IPDI-TMP-PPG-DEPD in red, IPDI-TMP-PPG-BD in blue and IPDI-TMP-PPG-PD in green].

Table 2
DSC data obtained during second heating scans of each MCPU-U containing IPDI and PPG.

Formulation	HS wt%	$T_g$sp/°C
PPG	–	−70
IPDI-TMP-PPG	33.8	−33
IPDI-TMP-PPG-DEPD	39.3	−32
IPDI-TMP-PPG-BD	37.7	−32
IPDI-TMP-PPG-PD	37.1	−33

HS = nominal hard-phase content, $T_g$sp = soft-phase glass transition temperature second heating scan.

3.2. ATR analysis

3.2.1. ATR of MDI-based adhesives

Within MCPU-U block copolymer systems, hydrogen-bonding plays a pivotal role in determining the final microphase morphology. It is noted that hydrogen-bonding is not the sole factor contributing towards final morphology but it will account for a significant portion. Common factors that influence MCPU-U morphology are phase compatibility, thermal history, stoichiometry etc. What is useful about hydrogen-bonding is that it shifts the position of both N–H and C=O vibrations. This makes it possible when interpreting both bands together, to gain further insight into what microstructure(s) are present within the polymer.

Table 3 contains selected assignments of possible interactions between N–H and C=O groups, complete with the wavenumber ranges in which they occur [14,21–23]. This table presents interactions of either free or hydrogen-bonded configurations which display varying degrees

Table 3
Typical infrared wavenumber ranges for N–H and C=O groups involved in hard-phase formation.

Functional Group	Wavenumber Range (cm^{-1})	Band Structure and Assignment	
Urethane/ Urea N–H	3600–3500	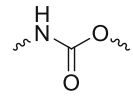	Free
Urethane/ Urea N–H	3360–3300	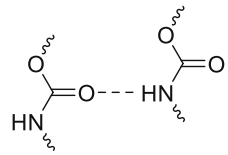	Hydrogen-Bonded
Urethane C=O	1740–1730	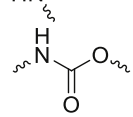	Free Urethane
Urethane C=O	1730–1710	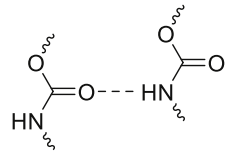	Hydrogen-Bonded Urethane
Urea C=O	1710–1690	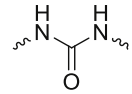	Free Urea
Urea C=O	1690–1655	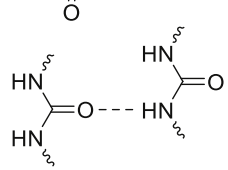	Monodentate Hydrogen-Bonded Urea
Urea C=O	1655–1620	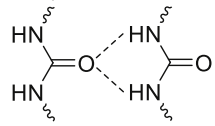	Bidentate Hydrogen-Bonded Urea

Table 4
Characteristic ATR bands obtained for each MDI MCPU-U synthesised with a different combination of chain-extenders.

	MDI-TMP-PPG	MDI-TMP-PPG-DEPD	MDI-TMP-PPG-BD	MDI-TMP-PPG-PD
Vibration	Wavenumber (cm^{-1})	Wavenumber (cm^{-1})	Wavenumber (cm^{-1})	Wavenumber (cm^{-1})
N–H stretching H-bonded	3341	3336	3334	3345
C–H stretching	2981	2971	2974	2980
C–H asymmetric stretch	2934	2928	2936	2936
C–H symmetric stretch	2876	2871	2871	2877
C=O stretch Urethane H-bonded	1715	1710	1710	1715
C=O stretch free Urea	1699	1700	1699	1700
C=O stretch Urea Bidentate H-bonded	1648	1640	1644	1644
C–N stretch, N–H bend	1530	1530	1535	1535
C–H bend aliphatic	1463	1463	1453	1453
C–H methyl deformation	1378	1373	1372	1367
C–N Urea	1340	1340	1350	1345
C–N Urethane	1307	1307	1306	1301
Asymmetric N–CO–O, C–H aliphatic skeleton	1231	1230	1246	1241
C–O–C stretch aliphatic ether	1093	1102	1094	1094
Symmetric N–CO–O	1016	1022	1017	1012
C–O–C stretch aliphatic ether	932	922	925	925
C–C skeleton vibration	866	870	870	865
C–C skeleton vibration	833	841	832	832
C–C skeleton rocking	775	775	778	772

of order/disorder. Omitted from the table are hydrogen-bonding interactions which occur within the soft-phase via the N–H group in phase mixed architectures. These groups have been omitted from the table as they are difficult to observe accurately. Table 4 lists the other principal peak assignments.

Fig. 4(a) displays the isolated N–H peaks from each of the four MCPU-U systems based on MDI and PPG. Contained within this N–H peak will be a combination of both urethane and urea in either free or hydrogen-bonded states. This peak also contains a weak carbonyl overtone between 3450 cm^{-1} – 3460 cm^{-1} [24]. From inspection of both N–H peak shape and position, it is clear that the hard-phase organisation is similar in all formulations, with the TMP only formulation displaying most variation. This observation is consistent with DSC analysis of these materials.

The position of peaks ascribed to hydrogen-bonded N–H groups are similar in each case, ranging between 3307 cm^{-1} – 3300 cm^{-1} (for values obtained from fitted data see Table 5). These hydrogen-bonding interactions are those of N–H groups within the hard-phase of the microstructure. Peak fitting was based around obtaining peak positions of hard-to-hard interactions; however, it is noted that within the peak area obtained there will be a contribution from hard-to-soft interactions. Evidence that hard-to-soft interactions are present can be observed in DSC data where both a broadened and elevated soft-phase glass transition temperature were observed (see section 3.1.2) because of phase-mixing.

Involvement of most N–H groups in hard-to-hard and hard-to-soft interactions is displayed by the small number of free groups available. The percentage of the peak area assigned to hydrogen-bonded N–H groups is greater than that of free N–H groups, which would be expected for a phase-mixed material. An example of the data obtained from deconvolution is shown within Fig. 4(b) for formulation MDI-TMP-PPG. The fit line obtained (red line) is the summation of the three fitted peaks used to detemine the free N–H, carbonyl overtone and hydrogen-bonded N–H (all deconvolution data available within supplementary information).

An advantage of using a polyether soft-phase such as PPG is that it allows for hard-phase carbonyl groups to be viewed exclusively without the complication of the ester carbonyls that would be present in a polyester soft-phase. Fitting of this carbonyl region used a similar procedure, with three peaks fitted to account for free urethane, hydrogen-bonded urethane and urea as shown in Table 5. The carbonyl peak for each adhesive is presented within Fig. 4 (c) and will contain a mixture of both urethane and urea moieties.

Peak shapes of the carbonyl region are similar in all four cases however, the TMP-only formulation has a larger tail at lower wavenumbers in comparison to each diol chain-extended formulations. This tail from urea carbonyl groups in the TMP-only formulation is inherent of the greater residual free isocyanate content which upon moisture cure will produce more urea-based groups. Urea carbonyls groups are observed between 1700 cm^{-1} – 1630 cm^{-1} and the above carbonyl positions are consistent with what would be expected based on a moisture cured system [24,25].

Deconvolution of this region has highlighted the different composition of carbonyl environments within each microphase structure. The amount of free urethane is similar regardless of chain-extender composition which is reflected in the tight range of 1733 cm^{-1} – 1728 cm^{-1} for this carbonyl type. Differences are observed however, in the hydrogen-bonded urethane range. For diol chain-extended formulations, the assigned peak area for hydrogen-bonded urethane ranges between 73%–76%. This amount of hydrogen-bonded urethane reduces to 61% in the TMP-only formulation.

This difference in hydrogen-bonded urethane will result from: (a) the diol chain-extended formulations having an inherent greater concentration of urethane groups and (b) the shift to lower wavenumbers of

Table 5
Data obtained from deconvolution of N–H and C=O peaks for MDI and PPG based MCPU-U adhesives using Gaussian fitting function.

Formulation	N–H (Ur + U)						C=O					
	Free		C=O Overtone		H-Bonded		Free Ur		H-bonded Ur		U	
	cm^{-1}	%	cm^{-1}	%	cm^{-1}	%	cm^{-1}	%	cm^{-1}	%	cm^{-1}	%
MDI-TMP-PPG	3523	9	3367	2.5	3312	89	1731	15	1716	61	1681	23.5
MDI-TMP-PPG-DEPD	3515	13.5	3373	11.5	3305	75	1732	16	1714	73	1678	11
MDI-TMP-PPG-BD	3530	9.5	3393	3.5	3308	87	1732	19	1711	76	1673	5
MDI-TMP-PPG-PD	3532	15	3374	9	3303	76	1732	15.5	1715	74	1680	10.5

Ur = urethane, U = urea.

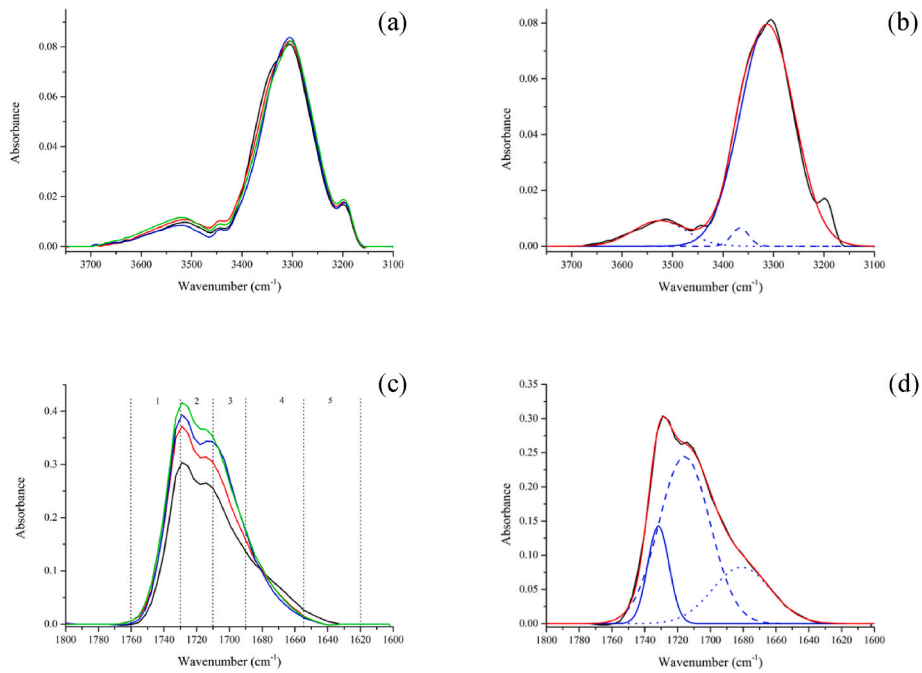

Fig. 4. ATR data collected from each MCPU-U adhesive. (a) Stacked N–H region, (b) deconvolution example of N–H region for MDI-TMP-PPG, (c) stacked C=O region and (d) deconvolution example of C=O region for MDI-TMP-PPG. [MDI-TMP-PPG in black, MDI-TMP-PPG-DEPD in red, MDI-TMP-PPG-BD in blue and MDI-TMP-PPG-PD in green].

carbonyl peak due to a greater amount of urea in TMP-only formulation. This is confirmed by the contribution of urea within the TMP-only formulation being double the value of each diol chain-extended formulation. These observations are consistent with what would be expected for diol chain-extended systems in the literature [14,21,22].

3.2.2. ATR of IPDI-based adhesives

Full peak assignment for each MCPU-U adhesive based on IPDI and PPG is presented within Table 6 To obtain additional information on microphase structure within each MCPU-U, deconvolution of N–H and C=O regions was performed. As shown in Fig. 5 (b), three components were extracted from the N–H region, hydrogen-bonded N–H (solid blue line), carbonyl overtone (dash blue line) and free N–H (dot blue line). Peak shapes of each MCPU-U are similar, with the most noticeable difference being additional free N–H in formulation IPDI-TMP-PPG-BD. This is mirrored in the ratio of hydrogen-bonded to free N–H being similar in each case. The ratios are as follows IPDI-TMP-PPG is 7.1:1, IPDI-TMP-PPG-DEPD is 6.1:1, IPDI-TMP-PPG-BD is 2.5:1 and IPDI-TMP-PPG-PD is 8.8:1.

Carbonyl regions of IPDI-based adhesives show that the hard-phase has a high degree of order (see Fig. 5 (c)). For each adhesive there are four types of carbonyl: hydrogen-bonded urethane, free urea, monodentate hydrogen-bonded urea and bi-dentate hydrogen-bonded urea. Other than free urea, all other interactions will be present within the hard-phase or hard-to-soft interactions and will act as physical reinforcement points for each adhesive matrix.

Deconvolution was performed by fitting four peaks to the carbonyl region to identify contributions from hydrogen-bonded urethane, free urea, monodentate hydrogen-bonded urea and bidentate hydrogen-bonded urea as shown in Fig. 5(d). The data obtained is summarised

Table 6
Characteristic ATR bands obtained for each IPDI MCPU-U synthesised with a different combination of chain-extenders.

	IPDI-TMP-PPG	IPDI-TMP-PPG-DEPD	IPDI-TMP-PPG-BD	IPDI-TMP-PPG-PD
Vibration	Wavenumber (cm^{-1})	Wavenumber (cm^{-1})	Wavenumber (cm^{-1})	Wavenumber (cm^{-1})
N–H stretching H-bonded	3341	3336	3334	3345
C–H stretching	2981	2971	2974	2980
C–H asymmetric stretch	2934	2928	2936	2936
C–H symmetric stretch	2876	2871	2871	2877
C=O stretch Urethane H-bonded	1715	1710	1710	1715
C=O stretch free Urea	1699	1700	1699	1700
C=O stretch Urea Bidentate H-bonded	1648	1640	1644	1644
C–N stretch, N–H bend	1530	1530	1535	1535
C–H bend aliphatic	1463	1463	1453	1453
C–H methyl deformation	1378	1373	1372	1367
C–N Urea	1340	1340	1350	1345
C–N Urethane	1307	1307	1306	1301
Asymmetric N–CO–O, C–H aliphatic skeleton	1231	1230	1246	1241
C–O–C stretch aliphatic ether	1093	1102	1094	1094
Symmetric N–CO–O	1016	1022	1017	1012
C–O–C stretch aliphatic ether	932	922	925	925
C–C skeleton vibration	866	870	870	865
C–C skeleton vibration	833	841	832	832
C–C skeleton rocking	775	775	778	772

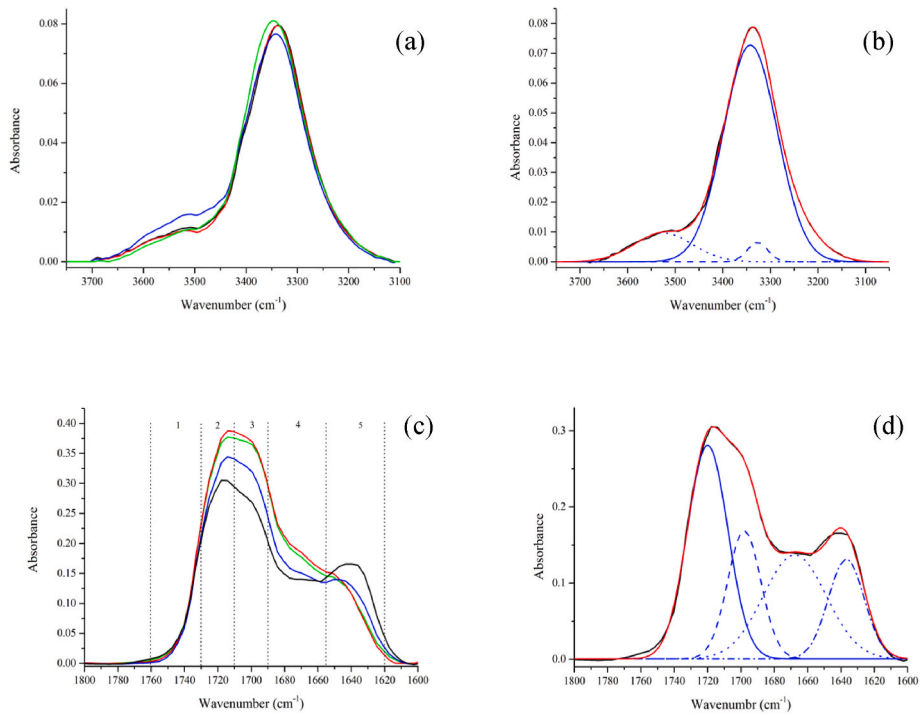

Fig. 5. ATR data collected from each MCPU-U adhesive. (a) Stacked N–H region, (b) deconvolution example of N–H region for IPDI-TMP-PPG, (c) stacked C=O region and (d) deconvolution example of C=O region for IPDI-TMP-PPG. [IPDI-TMP-PPG in black, IPDI-TMP-PPG-DEPD in red, IPDI-TMP-PPG-BD in blue and IPDI-TMP-PPG-PD in green].

in Table 7. In the TMP-only adhesive, a slightly larger proportion of bi-dentate urea is observed compared to each diol chain-extended formulation. As this adhesive contains more free isocyanate than diol chain-extended adhesives, this will result in the fully cured system having more urea containing groups. Formation of bi-dentate urea groups shows high order within the hard-phase and these ordered interactions are further evidence of phase separation. Bi-dentate urea groups are formed within all PPG-based adhesives and the lower viscosity within IPDI-based systems coupled with the slower cure time will promote their formation compared to MDI-based formulations.

3.3. Peel strength and haze

3.3.1. Peel strength and haze of MDI adhesives

Thermal and spectroscopic analysis has determined that this set of MCPU-U adhesives become more phase-separated with decreasing hard-phase content. Within the literature, it is stated that hard-segment contents of 50 wt% or greater result in microphase structures that are lamellar in nature with interweaving layers of both hard and soft-phases [19]. Within this set which contain MDI and PPG, the nominal hard-phase content is lower than 50 wt% and ranges from 36.4%–41.5 wt%, thus the expected microphase morphology will be more globular in nature, which will have an influence on final adhesive properties. This phase-separated or globular morphology will consist of hard-phase domains which are isolated from one another by soft-phase domains. These domains will be close to one another and as a result, the conformational constraints induced on the soft-phase will be great, resulting in a significant increase in the $T_g$sp as was observed using DSC.

Tested for each adhesive type were two laminate constructions, these contained either virgin polycarbonate or ethanolamine surface-treated polycarbonate [9]. When only TMP was used as chain-extender (MDI-TMP-PPG), failure was cohesive within the adhesive layer. For this adhesive type, peel strength values are greater for virgin polycarbonate compared to polycarbonate surface treated with ethanolamine. This may indicate that bonding via mechanical and attractive interactions with the substrate may occur over formation of covalent bonds [26]. Table 8 lists the peel strength and haze data obtained for each of the MCPU-U adhesives based on MDI and PPG.

Bond strength was at a maximum after 1 week for this formulation, with a reduction in peel strength observed after 1 month, however, this value remained stable after 18 months. Reductions in peel strength between 1 week and 1 month were 29% for PC(t)/PC(t) and 9% for PC/PC. This is further evidence that surface treatment has no beneficial impact on the peel strength observed for this adhesive type.

When diol chain-extended formulations were evaluated, mixed results were observed. Firstly, the mode of failure for each formulation was adhesive at the interface regardless of substrate combination. Secondly, recorded peel strength values are very much formulation

Table 7
Data obtained from deconvolution of N–H and C=O peaks for each IPDI and PPG based MCPU-U adhesive using Gaussian fitting function.

Formulation	N–H								C=O					
	Free		C=O Overtone		H-Bonded		H-Bonded Ur		Free U		Monodentate U		Bidentate U	
	cm^{-1}	%	cm^{-1}	%	cm^{-1}	%	cm^{-1}	%	cm^{-1}	%	cm^{-1}	%	cm^{-1}	%
1	3525	12	3421	3	3342	85	1719	39	1697	29	1672	16	1646	16
2	3516	14	3409	1	3337	85	1720	35	1698	34	1671	17	1646	14
3	3503	22	3407	1	3340	77	1721	33	1699	34	1669	19	1641	14
4	3536	10	3481	2	3345	88	1720	38	1698	29	1668	19	1637	14

Ur = urethane, U = urea, ***1*** = IPDI-TMP-PPG, **2** = IPDI-TMP-PPG-DEPD, **3** = IPDI-TMP-PPG-BD, **4** = IPDI-TMP-PPG-PD.

Table 8
Peel strength and haze data obtained for each MCPU-U adhesive based on MDI and PPG.

Adhesive Formulation	Laminate	Peel 1[x] (N mm^{-1})	Peel 2[y] (N mm^{-1})	Peel 3[z] (N mm^{-1})	Failure mode	Haze (%)
MDI-TMP-PPG	PC(t)/PC(t)	3.8	2.7	2.7	Cohesive	1.1%
	PC/PC	4.5	4.1	4.1	Cohesive	1.1%
MDI-TMP-PPG-DEPD	PC(t)/PC(t)	2.6	3.3	3.3	Adhesive	0.4%
	PC/PC	4.1	5.4	5.4	Adhesive	0.4%
MDI-TMP-PPG-BD	PC(t)/PC(t)	4.7	5.3	5.3	Adhesive	>1.5%
	PC/PC	ND	ND	ND	ND	ND
MDI-TMP-PPG-PD	PC(t)/PC(t)	1.1	1.1	1.0	Adhesive	>1.5%
	PC/PC	1.0	1.0	1.0	Adhesive	>1.5%

[x] Peel 1 collected within 1 week of room temperature cure, [y] peel 2 collected after 1 month of room temperature cure and [z] Peel 3 collected after 18 months of room temperature cure, ND = No Data.

Table 9
Peel strength and haze data obtained for each MCPU-U adhesive based on IPDI and PPG.

Adhesive Formulation	Laminate	Peel 1[x] (N mm^{-1})	Peel 2[y] (N mm^{-1})	Peel 3[z] (N mm^{-1})	Failure mode	Haze (%)
IPDI-TMP-PPG	PC(t)/PC(t)	4.8	6.0	4.9	Adhesive	0.5
	PC/PC	3.0	3.9	3.0	Adhesive	0.5
IPDI-TMP-PPG-DEPD	PC(t)/PC(t)	6.1	6.0	4.4	Adhesive	1.4
	PC/PC	4.7	3.2	3.4	Adhesive	0.7
IPDI-TMP-PPG-BD	PC(t)/PC(t)	1.5	3.4	2.5	Adhesive	0.8
	PC/PC	0.8	2.3	0.5	Adhesive	0.7
IPDI-TMP-PPG-PD	PC(t)/PC(t)	3.4	4.1	3.7	Adhesive	1.0
	PC/PC	2.9	3.4	3.0	Adhesive	0.3

[x] Peel 1 collected within 1 week of room temperature cure, [y] peel 2 collected after 1 month of room temperature cure and [z] Peel 3 collected after 18 months of room temperature cure.

dependent. Greatest peel strength was observed for formulation MDI-TMP-PPG-DEPD which had a measured peel strength of 5.4 N mm^{-1} after 18 months on virgin polycarbonate. A net increase in peel strength was observed from 1 week to 1 month by 27% for PC(t)/PC(t) and 32% for PC/PC. By increasing the degree of microphase mixing, it has promoted adhesion to the polycarbonate substrate, at the same time reducing haze.

For other formulations, poorer and less stable peel strengths were observed with the exception of MDI-TMP-PPG-BD within PC(t)/PC(t), where 5.3 N mm^{-1} was recorded after 18 months. These unstable tensile testing results are associated with observed foaming within the bond-line, with these bubbles also impacting obtained haze values. The root cause of this foaming is currently unknown and would require further investigation which was out-with the scope of this study. Therefore, the bond strength of these materials could not be accurately evaluated. The extent of bond-line foaming was not consistent - in MDI-TMP-PPG-BD within PC/PC, foaming was so excessive that a stable peel was never obtained and consequently no value could be assigned. Based on previous results obtained on similar systems, it would be anticipated that these materials would operate in a similar peel strength range as MDI-TMP-PPG-DEPD [8].

3.3.2. Peel strength and haze of IPDI adhesives

When using an aliphatic isocyanate, the observed morphology as characterised by DSC and ATR was more phase-separated than with the aromatic isocyanate. Greater phase-separation displays that the miscibility of IPDI with PPG is less than for MDI with PPG. This poorer miscibility is influenced by the greater steric effects associated with the isophorone ring structure. Table 9 lists the peel strength and haze data obtained for each of the MCPU-U adhesives based on IPDI and PPG.

For all formulations, unlike those observed for MDI-based formulation, surface treatment with ethanolamine has produced laminates of greater peel strength. Regardless of chain-extender formulation, the mode of failure was adhesive at the substrate interface. Greatest peel strength values obtained after 18 months of curing with 4.9 N mm^{-1} obtained for IPDI-TMP-PPG laminated between ethanolamine surface treated polycarbonate. The lowest peel strength value obtained was 0.5 N mm^{-1} for IDPI-TMP-PPG-BD laminated within PC/PC. As similar globular morphologies are present for each material as shown by DSC plus ATR analysis, it is anticipated that variations in peel strength are most likely to be process and not formulation related.

Formulations containing IPDI will cure at a slower rate due to the reduced reactivity of the aliphatic isocyanate groups. This was advantageous for haze as it reduced visible defects like bubble formation or foaming introduced to the laminate during cure. This makes haze values obtained for this adhesive set as a function of the microphase structure and not microphase structure plus curing defects as was the case for some of the MDI formulations. Lowest haze values were obtained for IPDI-TMP-PPG with a value of 0.5% obtained for PC(t)/PC(t) and PC/PC laminates. With the exception of IPDI-TMP-PPG-PD with PC/PC, haze values increased following diol chain-extension with the highest value of 1.4% obtained for IPDI-TMP-PPG-DEPD laminated within PC(t)/PC(t). Although haze is below the threshold value of 1.5% for all formulations tested, the relationship between microphase structure and haze is less clear.

3.4. Morphology model

With input from analysis in previous sections, it is possible to create morphology models to demonstrate changes to the microphase structure. These models will be used to demonstrate changes in microphase structure pre and post diol chain-extension. This will be related to what factors of the microphase structure are beneficial for peel strength and for adhesive haze.

Thermal and spectroscopic analysis was able to establish that the morphology of MDI-based adhesives was formulation dependent. Material properties and morphologies were significantly impacted by the presence of sterically hindered diol chain-extenders. TMP has a known disruptive effect on the hard-phase due to it triol structure [19]. When TMP was the sole chain extender, the morphology was of lower order with phase-mixing present. The globular morphology of this type is represented in Fig. 6(a). Mixing of the hard-phase with the soft-phase was demonstrated by observing the shift and broadening of the $T_g$sp. Further confirmation of phase-mixing was provided by ATR analysis through the peak positions of both N–H and C=O peaks.

Miscibility of hard and soft-phases in the MDI-based adhesives was significantly improved with the introduction of diol chain-extenders. Deployment by design of chain-extenders with steric groups promotes the migration of MDI-based hard-phase blocks into the soft-phase. The increased phase-mixing of both phases is represented by morphological models Fig. 6(b). Shifts in $T_g$sp between 9 °C and 15 °C were observed as a result of reduced hard-phase packing and subsequent mixing. ATR analysis reflected increased mixing by an observed shift of the carbonyl peak to lower wavenumbers and having a greater contribution from hydrogen-bonded urethane groups when diol chain-extenders are present.

Increasing the degree of phase-mixing i.e., going from Fig. 6(a)–(b) results in (i) hard-phase penetrating the soft-phase, thus becoming more disperse and (ii) hard-domains will be smaller with poor packing. For adhesion, increasing the degree of phase-mixing results in high peel

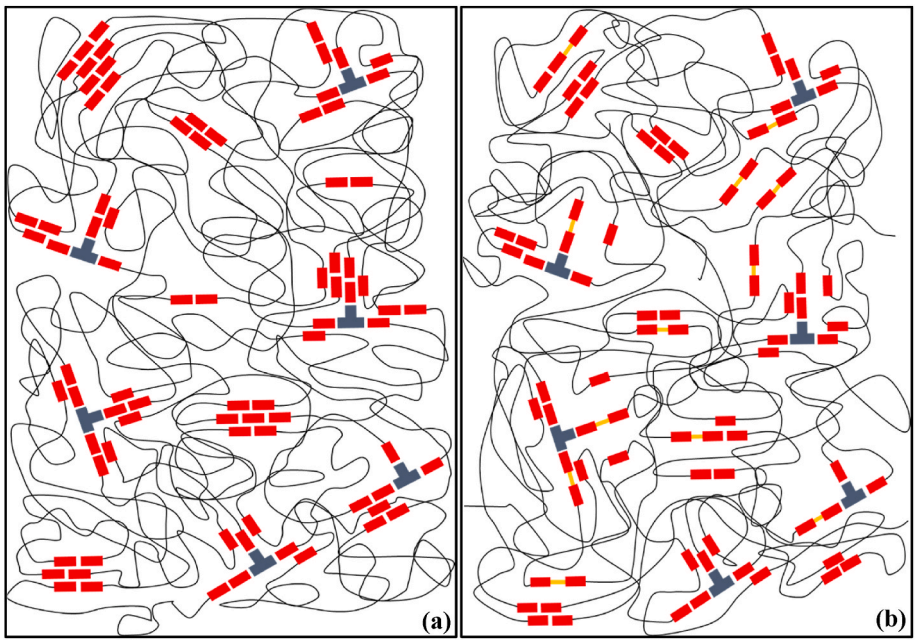

Fig. 6. Morphological models of MCPU-U for MDI and PPG adhesives. (a) Morphology in TMP only formulation and (b) morphology in diol chain-extended formulations. [Thin black line = amorphous soft-phase, red rectangle = MDI hard-phase, blue T-shape = TMP chain-extender and orange line = diol chain-extender].

strength values when processing defects were not encountered. Due to the planar structure of MDI aromatic rings, they are known to form well packed arrangements which makes selection of the chain-extender critical for obtaining low haze values as microphase domains >100 nm will start to scatter visible light. As the steric influence of the chain-extender combination increased, hard-phase/soft-phase mixing increased and recorded haze decreased, with the best performing combination being TMP plus DEPD for MDI-based formulations where no application issues were encountered. This is in contrast to the behaviour of IPDI based formulations, where phase mixing had minimal impact on haze and the haze value was more dependent on lower phase miscibility as evident in the $T_g$sp of the cured systems. This observation is consistent with prior work carried out on MCPU-U adhesives systems [8].

IPDI-based MCPU-U adhesives systems demonstrate a lower dependence on chain-extender composition in determining final microphase structure as demonstrated by Fig. 7(a) and (b). Upon introduction of a diol chain-extender, negligible change to $T_g$sp is observed. This indicates that hard-phase composition has minimal impact on the overall microphase structure due to the poor miscibility of IPDI and PPG. This was demonstrated by DSC, where all values of $T_g$sp were within 1 °C of one another.

A consequence of this immiscibility is that, overall, more ordered hard-phase architectures are obtained using IPDI. For a PPG-based system this can be observed through inspection of the carbonyl region

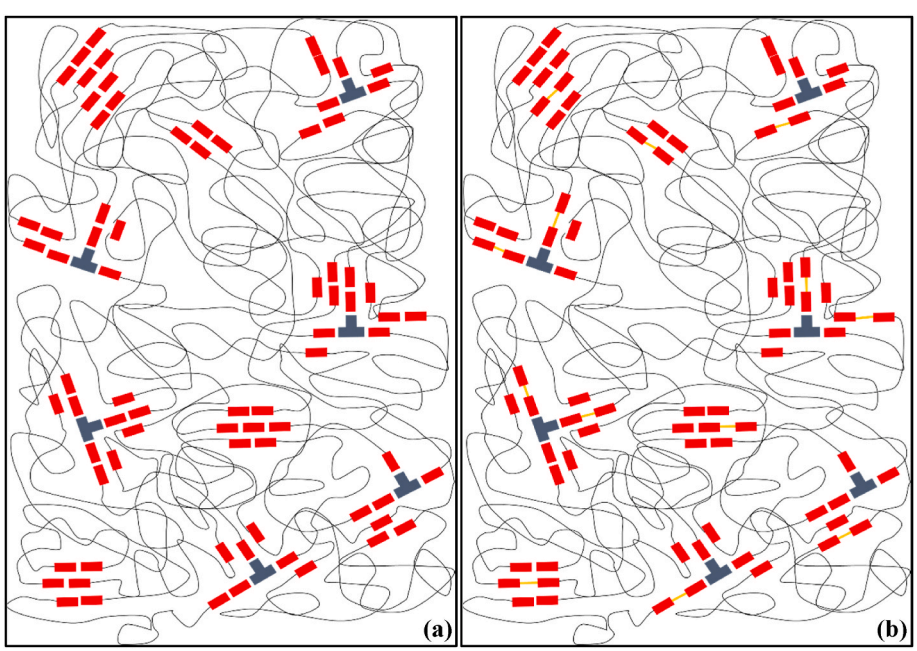

Fig. 7. Morphological models of MCPU-U for IPDI and PPG adhesives. (a) Morphology in TMP only formulation and (b) morphology in diol chain-extended formulations. [Thin black line = amorphous soft-phase, red rectangle = IPDI hard-phase, blue T-shape = TMP chain-extender and orange line = diol chain-extender].

which gives exclusive information on hard-phase order. For all IPDI-based adhesives, independent of formulation, highly ordered bi-dentate hydrogen-bonded urea was observed. The composition of this highly ordered moiety was greatest in the TMP-only formulation and reflects the greater free isocyanate content available during moisture cure. Even with the presence of sterically hindered chain-extenders, the combination of slower cure and phase immiscibility has transpired to deliver an ordered hard-phase.

With regards to peel strength and modes of failure, the obtained values plus behaviour did not greatly differ between compositions. This would be anticipated as altering the hard-phase has minimal impact on the global microphase structure. Poor miscibility and greater hard-phase order did influence the haze value obtained. Upon diol chain-extension regardless of combination, an increase in haze value was obtained. Diol chain-extension will increase the length of hard-blocks within the hard-phase. It has been demonstrated in the literature, that increasing hard-block length promotes hard-phase packing [20]. In the present study, chain-extension will interfere with the pack arrangement but will serve to increase block length which potentially will contribute to increased haze.

4. Conclusions

It has been demonstrated within this publication that MCPU-U adhesives are suitable candidates for lamination of flexible polycarbonate substrates. Selection of a soft-phase component devoid of crystallinity fosters the ability to produce adhesives with low haze contributions when hard-phase architecture is controlled. This is reflected in low haze values obtained for base formulations MDI-TMP-PPG and IPDI-TMP-PPG of 1.1% and 0.5% respectively.

Changes to microphase morphology following the introduction of sterically hindered diol chain-extenders were sensitive to isocyanate type. For MDI-based adhesives, hindered chain-extenders had a measurable effect on the morphology as evident by increased hard-phase/soft phase mixing. Of the chain-extenders, DEPD was the most sterically hindered and delivered the greatest improvement in phase-mixing. This was achieved with minimal compromise in peel performance. Adhesives of this design performed better when laminated with virgin polycarbonate film compared to ethanolamine treated film.

A separate scenario was presented for hard-phases that are IPDI-based, which are poorly miscible with PPG. Changes to hard-phase architecture had minimal impact on phase miscibility, and subsequently haze, as each IPDI-based formulation had a haze value of <1.5%. Addition of the chain-extenders did, however, contribute to a slightly less ordered hard-phase, as evident through the increased formation of mono-dentate hydrogen-bonded urea content in the ATR spectra. Furthermore, as the IPDI-based adhesives shared a similar globular morphology, each presented similar peel performance in terms of stability and strength. Adhesives of this type displayed improved peel performance during lamination with ethanolamine treated polycarbonate film compared to virgin polycarbonate film.

Acknowledgements

The authors would like to thank Dr P. L. Tang of Agilent Technologies for access to the infrared instrumentation and assistance during data processing. SM thanks Polaroid Eyewear for provision of a PhD studentship.

Appendix A. Supplementary data

Supplementary data to this article can be found online at https://doi.org/10.1016/j.ijadhadh.2022.103168.

References

[1] Su Q, Wei D, Dai W, Zhang Y, Xia Z. Designing a castor oil-based polyurethane as bioadhesive. Colloids Surf B Biointerfaces 2019;181:740–8. https://doi.org/10.1016/J.COLSURFB.2019.06.032.
[2] Berntsen JF, Morin D, Clausen AH, Langseth M. Experimental investigation and numerical modelling of the mechanical response of a semi-structural polyurethane adhesive. Int J Adhesion Adhes 2019;95:102395. https://doi.org/10.1016/J.IJADHADH.2019.102395.
[3] Somarathna HMCC, Raman SN, Mohotti D, Mutalib AA, Badri KH. The use of polyurethane for structural and infrastructural engineering applications: a state-of-the-art review. Construct Build Mater 2018;190:995–1014. https://doi.org/10.1016/J.CONBUILDMAT.2018.09.166.
[4] Srichatrapimuk VW, Cooper SL. Infrared thermal analysis of polyurethane block polymers. J Macromol Sci Part B 1978;15(2):267–311. https://doi.org/10.1080/00222347808212599.
[5] Golling FE, Pires R, Hecking A, Weikard J, Richter F, Danielmeier K, Dijkstra D. Polyurethanes for coatings and adhesives – chemistry and applications. Polym Int 2019;68(5):848–55. https://doi.org/10.1002/pi.5665.
[6] Watts JF, Critchlow GW, Packham DE, Kneafsey B, Sherriff M, Shanahan MER, Cope BC, Pascoe MW, Sagar AJG, Allen KW, et al. Adhesive classifications. In: Handbook of adhesion. Wiley Online Books; 2005. p. 26. https://doi.org/10.1002/0470014229.ch1.
[7] Sargent JP, Tredwell S, Dixon DG, Buxton AL, Shanahan MER, Padday JF, Pizzi A, Paxton BH. Wetting kinetics. In: Handbook of adhesion. Wiley Online Books; 2005. p. 599. https://doi.org/10.1002/0470014229.ch21.
[8] McCreath S, Boinard P, Boinard E, Gritter P, Liggat JJ. High clarity poly (Caprolactone Diol)-based polyurethane adhesives for polycarbonate lamination: effect of isocyanate and chain-extender. Int J Adhesion Adhes 2018;86:84–97. https://doi.org/10.1016/J.IJADHADH.2018.08.003.
[9] Li C, Wilkes GL. The mechanism for 3-aminopropyltriethoxysilane to strengthen the interface of polycarbonate substrates with hybrid organic-inorganic sol-gel coatings. J Inorg Organomet Polym 1997;7(4):203–16. https://doi.org/10.1023/A:1021690423544.
[10] Cowie JMG, Arrighi V. Step-growth polymerization. In: Polymers: chemistry and physics of modern materials; 2007. p. 29–56.
[11] Cowie JMG, Arrighi V. Chapter 12. The glassy state and glass transition. In: Polymer chemistry and physics of modern materials; 2007. p. 321–43.
[12] Yingjie L, Gao T, Liu J, Linliu K, Deeper CR, Chu B. Multiphase structure of a segmented polyurethane: effects of temperature and annealing. Macromolecules 1992;25(26):7365–72. https://doi.org/10.1021/ma00052a045.
[13] Šebenik U, Krajnc M. Influence of the soft segment length and content on the synthesis and properties of isocyanate-terminated urethane prepolymers. Int J Adhesion Adhes 2007;27(7):527–35. https://doi.org/10.1016/j.ijadhadh.2006.10.001.
[14] Li W, Ryan AJ, Meier IK. Effect of chain extenders on the morphology development in flexible polyurethane foam. Macromolecules 2002;35(16):6306–12. https://doi.org/10.1021/ma020231l.
[15] Sanchez-Adsuar MS, Martín-Martínez JM. Influence of the length of the chain extender on the properties of thermoplastic polyurethanes. J Adhes Sci Technol 1997;11(8):1077–87. https://doi.org/10.1163/156856197X00840.
[16] Gisselfält K, Helgee B. Effect of soft segment length and chain extender structure on phase separation and morphology in poly(urethane urea)S. Macromol Mater Eng 2003;288(3):265–71. https://doi.org/10.1002/mame.200390023.
[17] Martin DJ, Meijs GF, Gunatillake PA, Mccarthy SJ, Renwick GM. The effect of average soft segment length on morphology and properties of a series of polyurethane elastomers. II. SAXS-DSC annealing study. J Appl Polym Sci 1997;64(4):803–17. https://doi.org/10.1002/(SICI)1097-4628(19970425)64:4<803::AID-APP20>3.0.CO;2-T.
[18] Clau S, Dijkstra DJ, Gabriel J, Kläusler O, Matner M, Meckel W, Niemz P. Influence of the chemical structure of PUR prepolymers on thermal stability. Int J Adhesion Adhes 2011;31(6):513–23. https://doi.org/10.1016/j.ijadhadh.2011.05.005.
[19] Petrović ZS, Javni I, Divjaković V. Structure and physical properties of segmented polyurethane elastomers containing chemical crosslinks in the hard segment. J Polym Sci Part B Polym Phys 1998;36(2):221–35. https://doi.org/10.1002/(SICI)1099-0488(19980130)36:2<221::AID-POLB3>3.0.CO;2-U.
[20] Koberetein JT, Leung7 LM. Compression-molded polyurethane block copolymers. 2, 25. Evaluation of Microphase Compositions; 1992.
[21] Daniel-da-Silva AL, Bordado JCM, Martín-Martínez JM. Moisture curing kinetics of isocyanate ended urethane quasi-prepolymers monitored by IR spectroscopy and DSC. J Appl Polym Sci 2008;107(2):700–9. https://doi.org/10.1002/app.26453.
[22] Elwell MJ, Ryan AJ, Grünbauer HJM, Lieshout H C Van. An FT i.r. Study of reaction kinetics and structure development in model flexible polyurethane foam systems. Polymer (Guildf). 1996;37(8):1353–61. https://doi.org/10.1016/0032-3861(96)81132-3.
[23] Elwell MJ, Ryan AJ, Grünbauer HJM, Van Lieshout HC. In-situ studies of structure development during the reactive processing of model flexible polyurethane foam systems using FT-IR spectroscopy, synchrotron SAXS, and rheology. Macromolecules 1996;29(8):2960–8. https://doi.org/10.1021/ma9511208.
[24] Yılgör E, Yılgör İ, Yurtsever E. Hydrogen bonding and polyurethane morphology. I. Quantum mechanical calculations of hydrogen bond energies and vibrational

spectroscopy of model compounds. Polymer (Guildf). 2002;43(24):6551–9. https://doi.org/10.1016/S0032-3861(02)00567-0.

[25] Yilgör E, Yurtsever E, Yilgör I. Hydrogen bonding and polyurethane morphology. II. Spectroscopic, thermal and crystallization behavior of polyether blends with 1,3-dimethylurea and a model urethane compound. Polymer (Guildf) 2002;43(24): 6561–8. https://doi.org/10.1016/S0032-3861(02)00566-9.

[26] Watts, J. F.; Critchlow, G. W.; Packham, D. E.; Kneafsey, B.; Sherriff, M.; Shanahan, M. E. R.; Cope, B. C.; Pascoe, M. W.; Sagar, A. J. G.; Allen, K. W.; et al. A. In handbook of adhesion; John Wiley & Sons, Ltd, 2005; pp 1–58. https://doi.org/10.1002/0470014229.ch1.